Eur. Phys. J. D **25**, 139–148 (2003)
DOI: 10.1140/epjd/e2003-00093-9

THE EUROPEAN PHYSICAL JOURNAL D

Power-law decay of collisionally excited amino acids and quenching by radiative cooling

J.U. Andersen[1,a], H. Cederquist[2], J.S. Forster[3], B.A. Huber[4], P. Hvelplund[1], J. Jensen[2], B. Liu[1], B. Manil[4], L. Maunoury[4], S. Brøndsted Nielsen[1], U.V. Pedersen[1], H.T. Schmidt[2], S. Tomita[1], and H. Zettergren[2]

[1] Dept. of Physics and Astronomy, University of Aarhus, 8000 Århus C, Denmark
[2] Physics Dept., Stockholm University, SCFAB, 106 91 Stockholm, Sweden
[3] Département de Physique, Université de Montréal, Montréal, Québec, H3C 317 Canada
[4] Centre Interdisciplinaire de Recherche Ions Lasers, rue Claude Bloch, B.P. 5133, 14070 Caen Cedex 5, France

Received 12 December 2002 / Received in final form 27 February 2003
Published online 29 April 2003 –

Abstract. We have investigated the time dependence of the fragmentation of protonated amino acids stored at 22 keV in the electrostatic ring ELISA. The ions were produced in an electrospray source and after bunching in a quadrupole trap they were excited by collisions in a Ne gas. As in earlier studies of metal clusters and fullerenes produced in "hot" ion sources we find that the dissociation of metastable molecules follows approximately a $1/t$ decay law until a time τ after which the yield falls off much more rapidly. We interpret this reduction as a result of radiative cooling with a characteristic cooling time, $\tau_c \simeq G\tau$, where G is the magnitude of the exponent in an Arrhenius expression for the rate of the dominant fragmentation process. The values of τ obtained from fits to the data are in the range 9–17 ms corresponding to cooling times of a few hundred milliseconds, in good accord with the expected rate of cooling by emission from IR-active vibrations. The power-law behaviour for $t < \tau$ varies somewhat between the different amino acids, with powers between -0.9 and -1.1. We argue that this may be due to a competition between fragmentation channels with different Arrhenius parameters.

PACS. 82.39.-k Chemical kinetics in biological systems – 82.40.-g Chemical kinetics and reactions: special regimes and techniques – 87.15.-v Biomolecules: structure and physical properties

1 Introduction

We have investigated the time dependence of collision induced dissociation of protonated amino acids. A basic question in studies of the dynamics of excited molecules or clusters is whether the process is ergodic, *i.e.*, whether the excitation energy is distributed statistically over all degrees of freedom before the decay. Direct and ergodic processes usually take place on very different time scales. At not too high excitation energies the heat capacity is dominated by vibrations, and the coupling from electronic excitation to the vibrational heat bath typically requires pico- to nanoseconds [1,2]. When, as here, the excitation couples the energy directly into nuclear motion and the decay is measured on a time scale of micro- to milliseconds there should be ample time for equilibration.

A storage ring is well suited for such measurements. It covers a large time range, from the microsecond revolution time to the storage time of several seconds, and the large kinetic energy of the ions makes it easy to detect fragmentation or particle emission since the neutral decay products move in the forward direction and give a big signal in a particle counter. The ions are injected into the ring from a source that ideally delivers a short bunch of cold molecular ions, which can then be excited to a well defined internal energy by photon absorption in the ring. As we have demonstrated by an investigation of fullerene anions [3], such measurements can provide detailed information about the decay parameters. Also for molecules of biological importance they may become a useful supplement to the now standard method of threshold measurements of collision induced dissociation [4].

However, it can be difficult to add a well defined excitation energy. Photon absorption is often limited to narrow bands, as it is the case for the amino acids under investigation here, and therefore it may not be possible to reach the relevant excitation energies by absorption of a single photon. After multi-photon absorption or other excitation processes like electron impact or collisions in a gas there is a considerable spread in excitation energy. Moreover, most conventional ion sources such as sputter sources or plasma sources deliver beams of ions with large and poorly defined internal excitation. It is therefore of interest to investigate which information can be obtained

[a] e-mail: jua@ifa.au.dk

from measurements on ions with a broad distribution in internal energy (or temperature).

For such an ensemble the time dependence of the decay rate is determined by depletion of the hottest molecules, and we have demonstrated earlier that it follows a power law t^n with a power close to $n = -1$ [5]. In contrast to the exponential dependence a power law does not contain any characteristic time and hence little is apparently learned about the reaction, except that the decay rate is a strongly increasing function of temperature. However, if there are several decay channels the temperature dependent competition between these may be revealed by a change in the power n. As an example, the measurements in [6] of electron emission from C_{60} in competition with dissociation by C_2 emission provided the first clear experimental evidence that the dissociation energy for this molecule is much higher than derived from earlier experiments.

The measurement may also provide a clear signature of radiative cooling. Photon emission is always a competing process and the decay channel under observation, for example fragmentation or electron emission, may be quenched by radiative cooling. This leads to an exponential cut-off of the $1/t$ distribution at a characteristic quenching time τ [5]. In measurements on isolated systems with well defined excitation energy the lifetime must be shorter than the quenching time for the experiment to give information about the parameters of the decay. For lower excitation energies and longer lifetimes the decay can only be studied by measurements on systems in thermal equilibrium with a heat bath, maintained for example by emission and absorption of heat radiation [7–9] or by gas collisions [10].

For metal clusters the coupling to the radiation field is normally dominated by the plasma resonance [11–13] and also for large molecules like the fullerenes the power of the radiation at high temperatures may be derived from a plasma model [14]. For smaller molecules discrete electronic transitions dominate at high temperatures [15]. However, most chemical reactions take place at lower temperatures where the electronic excitations are frozen out, and the heat radiation then consists mainly of the discrete lines from IR (infra-red) active vibrations. There is an extensive literature on the influence of such radiation on chemical reactions, especially by Dunbar and coworkers [16].

Previously, we have determined quenching times from storage ring experiments for systems cooled by electronic transitions, both metal clusters and fullerenes [5,17,18]. Here we extend the measurements to molecules which are cooled mainly by emission from vibrations, and we have studied the amino acids, which are the building blocks of peptides and proteins. Protonated amino acids were produced in an electrospray source and bunched in an ion trap, and just after extraction from the trap they were excited by collisions in a Ne gas.

There are 20 amino acids which occur commonly in proteins. The protonated form of the simplest amino acid, glycine, has the structure $^+NH_3$–CH_2–COOH while the others have one hydrogen atom in the central CH_2 group replaced by a larger side chain. The dynamic properties of the molecules are expected to depend on the size and structure of this side chain. The seven protonated amino acids we have investigated can be divided into three groups: the two smallest molecules, glycine and alanine with a side chain consisting of just a CH_3 group, two molecules with a long linear side chain, where the proton is residing, arginine and lysine, and three molecules with a side chain containing an aromatic ring, phenylalanine, tyrosine and tryptophan.

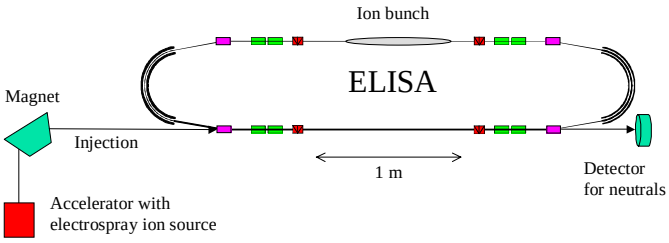

Fig. 1. The electrostatic storage ring ELISA. A pulse of ions is injected from the lower left at 22 keV energy. Neutrals are detected turn by turn with a micro-channel plate at the lower right.

For all the molecules investigated the decay is found to follow approximately a power law t^n at short times, with n varying from about -0.9 to -1.1. We discuss various corrections to the power law and demonstrate by a model calculation that the observed variation in n may be related to a temperature dependent competition between decay channels with different Arrhenius parameters. At times longer than 10–20 ms the power-law is replaced by a more rapid decrease, which can be modelled as exponential quenching by radiative cooling.

2 Experiment

The measurements were carried out at the storage ring ELISA (**El**ectrostatic **I**on **S**torage ring, **A**arhus) [18,19]. It is particularly useful for the study of very heavy molecules because all the optical elements are electrostatic and hence the ion trajectories depend only on energy and charge. As illustrated in Figure 1, the ring consists of two straight sections about 3 m long, and the ions are deflected by 180° at the ends. Typically, a bunch of ions is injected every 100 ms, and neutrals produced by unimolecular decay or by collisions with the rest gas are recorded by a micro-channel-plate detector. The injection voltage is 22 kV and for singly charged amino acids with masses of order 100 amu the revolution time is of order 40 μs. The phase space for stable storage is rather large but — depending on the injection conditions — there can be a small reduction of the ion current during the first few tens of revolutions. The pressure in the ring is a few times 10^{-11} mbar and collisions with the rest gas limit the storage lifetime to about 10 s.

A schematic drawing of the ion source is shown in Figure 2. Protonated amino acids (singly charged) were produced from a water-methanol solution (1% acetic acid)

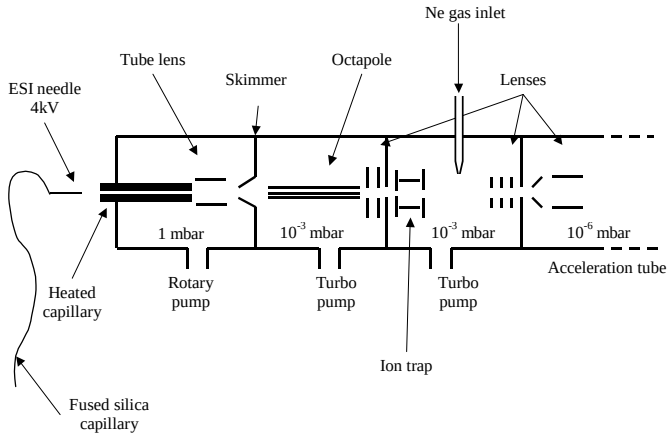

Fig. 2. The electrospray ion source and the ion trap for bunching of the ions. The buffer gas in the trap is helium but neon is let into the chamber to provide collisional excitation of extracted ions.

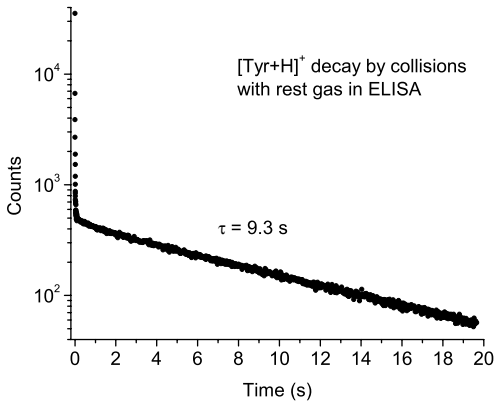

Fig. 3. Time spectrum for 20 s storage of protonated tyrosine. Except for the first fraction of a second, the yield of neutrals is dominated by dissociation induced by collisions with the rest gas, and the exponential decrease of the signal corresponds to the reduction of the number of stored ions.

with a home-built electrospray ion source. The solution is sprayed from a needle with a positive potential of about 4 kV and the positively charged droplets are transmitted through a heated capillary (180 °C) into the first vacuum chamber with a pressure of about 1 mbar. This process produces desolvated cations of the protonated amino acid. The ions are guided by the field from a tube lens through a skimmer into the next chamber with a pressure of about 10^{-3} mbar, and further by an octapole ion guide into the third chamber where they are stored in a cylindrical quadrupole trap with a He trapping gas at a pressure of about 10^{-3} mbar. The ions are extracted from the trap as a pulse of a few μs for injection into ELISA. Before injection they are focussed by an Einzel lens, accelerated by a 22 kV potential, and mass selected with a magnet.

In order to produce a broad spectrum of excitation we introduced Ne gas into the last chamber, as illustrated in the figure. We also tried heavier gases, Ar and Xe, but they were found not to be more effective. After extraction by ±15 V potentials on the ends of the trap the ions are accelerated towards the Einzel lens with a potential on the first lens of about −300 V, and during this acceleration they may collide with Ne atoms. Even for the heaviest ions, tryptophan with mass number 205, the centre-of-mass energy in collisions with Ne can be up to more than 25 eV, and the collisions should therefore lead to a long tail in the distribution in internal energy, stretching to energies where the dissociation lifetime is very short. Collisional excitation in the ion source, mainly in the first chamber, is "forgotten" in the trap, where the ions equilibrate with the room temperature He gas. However, there can be excitation in the trap due to the micro-motion induced by the RF field, especially if the trap is filled so that ions are pushed from the centre by the space charge potential [21]. To control the degree of filling of the trap we therefore introduced a stop voltage on the skimmer at a variable time after ion extraction, and we checked that the observed time dependence of the decay in ELISA was independent of the length of the filling period (10–100 ms).

With Ne in the trap instead of He there is more heating due to micro-motion and a dependence of the time spectrum on the trapping time was indeed observed. We therefore kept He as the buffer gas and introduced Ne only through the separate inlet indicated in Figure 2.

3 Results

The neutral fragments originate partly from decay of metastable molecules, partly from collisions with the rest gas in the ring. Gas collisions dominate at long times, as illustrated by the spectrum in Figure 3, recorded with an injection rate of 0.05 Hz. The yield from decay of metastable molecules is visible only during the first fraction of a second and the rest of the spectrum shows an exponential depletion of the beam by gas collisions, with a lifetime of 9.3 s. This depletion is negligible for the spectra presented in the following, with a maximum storage time of 80 ms, and in the analysis the yield of neutrals from gas collisions can be approximated by a constant. Excitation by collisions without immediate dissociation should be negligible.

In Figure 4 the results for phenylalanine are shown both in a log-log plot and in a semilog plot to illustrate the analysis in detail. The logarithmic time scale in Figure 4a is useful for observation of the power-law behaviour, and up to about 10 ms the yield follows closely the $1/t$ dependence given by the dashed curve. The yield is then strongly reduced owing to radiative cooling and, as illustrated more clearly in Figure 4b with the linear time scale, it approaches a constant value corresponding to fragmentation by gas collisions. Based on the theoretical discussion in the following section (see Eq. (12)) we have fitted the spectra by the function,

$$I(t) = N\,(t/\tau)^{\delta}\left(\mathrm{e}^{t/\tau}-1\right)^{-1} + K. \qquad (1)$$

Here N is a normalisation constant and the factor $(t/\tau)^{\delta}$ corrects the effective power in the power law t^n at short

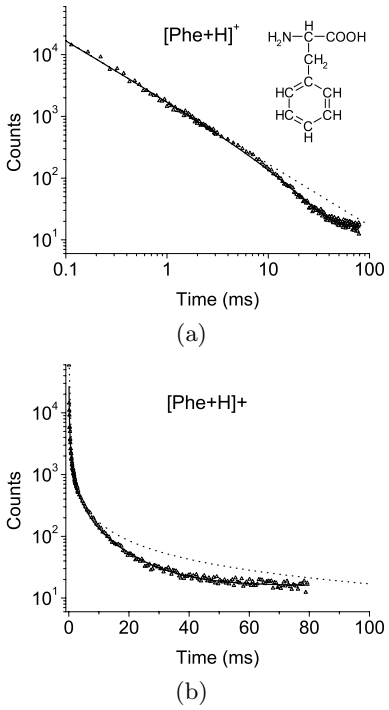

Fig. 4. Time spectrum for 100 ms storage of protonated phenylalanine. For $t > 3$ ms the yield of neutrals is averaged over 10 revolutions. The initial rapidly decreasing signal is due to decay of the hottest molecules and after 10 ms this signal is quenched by radiative cooling. The dashed line in the log-log plot in (a) is proportional to $1/t$ while the solid curve is a fit with the expression in equation (1) with the parameters given in Table 1. The approach to the constant yield from gas collisions is seen more clearly in the semilog plot in (b). The structure illustrated in (a) is for the neutral amino acid.

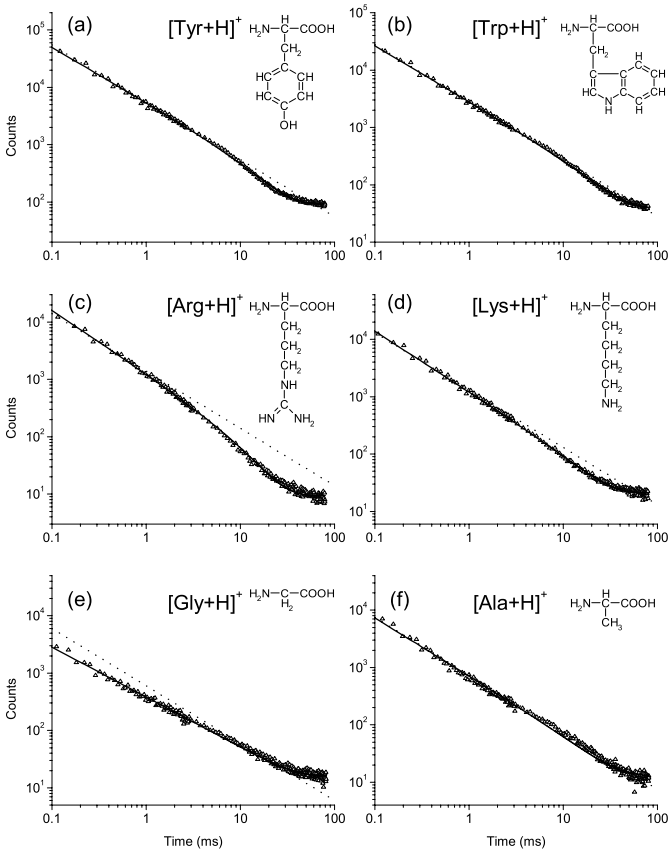

Fig. 5. As Figure 4a but for tyrosine (a), tryptophan (b), arginine (c), lysine (d), glycine (e) and alanine (f).

times ($t < \tau$) to $n = -1+\delta$, while the additive constant K accounts for fragmentation by collisions in the ring. The most important parameter is the quenching time τ which is to be determined by the experiment. The resulting fit is shown as the full drawn curve in Figure 4, and the fitting parameters are given in Table 1 for all the molecules investigated.

The results obtained for two similar amino acids, tyrosine and tryptophan, are shown in Figures 5a and 5b. As illustrated in the figures, all three molecules have side chains containing an aromatic ring. The results and the parameters derived are also quite similar. The two molecules illustrated in Figures 5c and 5d, arginine and lysine, have also rather large but linear side chains. As seen in Table 1, the slopes are slightly steeper, in particular for arginine, but the characteristic quenching times are very similar to the results for the other molecules. Figures 5e and 5f show the results for the two smallest amino acids, glycine and alanine. The data for alanine are rather similar to those for the first group of molecules but for glycine the logarithmic slope is somewhat less steep. The background of fragmentation in rest-gas collisions is relatively higher for these small molecules and the quenching by cooling is hardly visible. The values for τ are therefore not well determined and they have been fixed at 15 ms. The fit for alanine is clearly not very good; we discuss possible reasons for this below and present an alternative fit in Figure 8.

Table 1. The molecular weights of the protonated amino acids and the parameters in equation (1) used to fit the observed time dependence of collision induced dissociation, as illustrated in Figures 4 and 5. The power n in the power law at short times is given by $n = -1 + \delta$. The values of τ are not well determined for glycine and alanine and have been fixed at 15 ms; the uncertainty in τ is estimated to be about 3 ms for the other molecules.

Molecule	N	$N/10^3$	δ	τ (ms)	K
Phe+H$^+$	144	23.1	0.02	13	17
Tyr+H$^+$	549	67.5	0.04	11	95
Trp+H$^+$	179	51.3	0.03	17	41
Arg+H$^+$	115	9.1	−0.10	9	9
Lys+H$^+$	87	13.6	−0.05	13	21
Gly+H$^+$	36	0.54	0.13	(15)	16
Ala+H$^+$	46	0.70	−0.01	(15)	13

4 Analysis and discussion

In analogy with earlier measurements [5], we interpret the initial rapid decay of stored ions as statistical fragmentation of molecules injected with high internal energy. A paradigm for the description of statistical decay is Bohr's compound nucleus introduced to account for disintegration of heavy nuclei after neutron absorption [22]. The excitation energy is assumed to spread over the available states so that all states with this energy are populated with equal probability. The decay rate is then independent of the mode of excitation and can be expressed in terms of the level density of the system [23–25].

4.1 Microcanonical temperature and heat capacity

For molecules in a container at temperature T, the rate constant for dissociation with activation energy E_d can be expressed by the Arrhenius formula as a Boltzmann factor multiplied by a frequency which varies slowly with temperature,

$$k = v \exp\left(\frac{-E_d}{k_B T}\right). \tag{2}$$

The magnitude of the exponent plays an important role in the following analysis, and we denote this quantity by the symbol G ("Gspann parameter") as it is customary in statistical analysis of cluster decay. Typically, the value of G is in the range 10–30.

Since we are here concerned with the decay of isolated systems with conserved internal energy E, the relevant temperature concept is the microcanonical temperature defined in terms of the derivative of the logarithm of the level density, $1/k_B T \equiv \mathrm{d}/\mathrm{d}E \ln \rho(E)$. The microcanonical decay rate can be expressed in Arrhenius form with an effective decay temperature, T_e, given by

$$T_e = T - \frac{E_d}{2C} - \frac{E_d^2}{12C^2 T}, \tag{3}$$

where T is the temperature before the decay and C is the microcanonical heat capacity at energy $E - E_d/2$. The expression in equation (3) may be derived from a Taylor expansion of the logarithm of the level density at this energy [26,27]. The same expression was obtained by Klots in his finite-heat-bath theory but on a different conceptual basis [28]. For very large molecules only the first order correction needs be retained and the effective temperature is then the average of the temperatures in the initial and final states. We shall use this approximation below. The correction to T is called the finite-heat-bath correction. If the frequency factor v is temperature dependent it should be evaluated at the temperature of the final state, $T_f = T - E_d/C$ [27]. The heat capacity C is approximately equal to the canonical heat capacity minus Boltzmann's constant k_B and may therefore easily be evaluated in the harmonic approximation from calculated vibrational frequencies [26]. Such a calculation for tryptophan is described in a later section and the resulting caloric curve is shown in Figure 6.

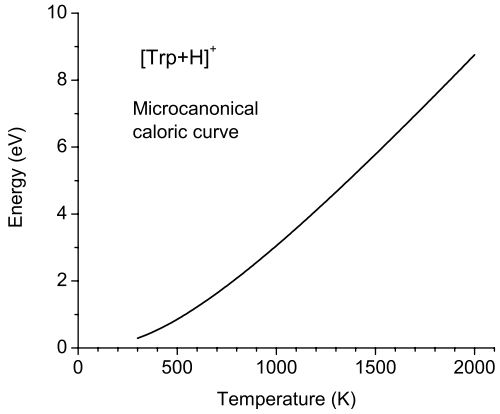

Fig. 6. Microcanonical caloric curve for tryptophan, calculated in the harmonic approximation from the vibrational frequencies obtained from a density functional calculation. The heat capacity was assumed to be equal to the canonical value minus k_B [26].

4.2 $1/t$ decay law

Following the analysis in reference [5] we now consider the decay of an ensemble of isolated molecules with a distribution $g(E)$ in excitation energy at the time $t = 0$ when the ensemble was created. In statistical equilibrium the rate constant k for the decay depends only on the energy and the angular momentum, and usually the latter can be ignored (see, for example, the discussion of this point in [27]). If E is conserved for individual molecules, the energy distribution decays exponentially and the fragmentation yield at time t is given by

$$I(t) = \int \mathrm{d}E\, g(E)\, k(E) \exp(-k(E)t). \tag{4}$$

Since $k(E)$ is a rapidly increasing function the weight function $k \exp(-kt)$ in equation (4) exhibits a sharp maximum at an energy E_m where $k = 1/t$, and this leads to an approximate $1/t$ dependence of $I(t)$ for decay of molecules with a broad energy distribution. One way to derive this dependence is to note that the function $k'(E)t \exp(-k(E)t)$ is minus the derivative of the exponential function and hence integrates to unity. Introducing this function into equation (4) and evaluating slowly varying factors at E_m we obtain

$$I(t) \simeq \frac{1}{t} g(E_m) \left(\frac{k(E_m)}{k'(E_m)}\right). \tag{5}$$

The last two factors vary slowly with time and we have approximately $I(t) \propto 1/t$.

For the following discussion it is useful to derive this formula in a slightly different way, which leads to a simple interpretation of the last factor in equation (5). As noted above, the function $k(E) \exp(-k(E)t)$ peaks sharply at the energy E_m where $k = 1/t$, and we may approximate the function by a Gaussian, $(\mathrm{e}^{-1}/t) \exp(-(E-E_m)^2/2\sigma^2)$. Equating the second derivatives at E_m of the two functions we find that σ equals the last factor in equation (5).

This equation is then obtained from an evaluation of the integral in equation (4) as $g(E_m)$ multiplied by the area of the Gaussian, with the approximation $(2\pi)^{1/2}\mathrm{e}^{-1} \simeq 1$.

As seen in Figure 5 and in Table 1, all the observations are consistent with the prediction of a power-law decay at early times, with a power n close to -1. However, there are significant variations in the value of n and these may contain interesting information on the dissociation dynamics. To investigate this question we first consider various small corrections to the power law and then we turn to the analysis of quenching by radiative cooling.

4.3 Corrections to the power $n = -1$ in the decay law

For a more detailed discussion it is useful to introduce the microcanonical temperature and the Arrhenius form of the rate constant. We denote by $T_{e,m}$ the value of the effective decay temperature T_e corresponding to E_m and obtain

$$I(t) \simeq \frac{1}{t} g(E_m) C(E_m) \frac{k_B T_{e,m}^2}{E_d}, \tag{6}$$

where we have ignored the temperature dependence of the pre-exponential factor v in the Arrhenius formula and used the approximation $\mathrm{d}E/\mathrm{d}T_e \simeq C(E)$.

We now evaluate the contributions to n from the individual factors in equation (6) by logarithmic differentiation, for example for the first factor: $\mathrm{d}(\ln(1/t))/\mathrm{d}\ln(t) = -1$. The contribution from $T_{e,m}^2$ is obtained from equation (2) and the relation $k(E_m) = 1/t$,

$$\frac{\mathrm{d}\left(\ln\left(T_{e,m}^2\right)\right)}{\mathrm{d}(\ln(t))} = -\frac{2\mathrm{d}(\ln(\ln(vt)))}{\mathrm{d}(\ln(t))} = \frac{-2}{\ln(vt)} = \frac{-2}{G}. \tag{7}$$

The vibrational heat capacity is also an increasing function of energy or temperature but it approaches an asymptotic value at high temperatures (see Fig. 6). At temperatures just below 1000 K it scales with a fairly low power of $T_{e,m}$, approximately as $C \propto T_{e,m}^{0.4}$, and hence the contribution to n from this factor is small, of order $-0.4/G$.

For a flat distribution in energy the power should then be $n \simeq -1.1$ but the logarithmic slope is reduced by the factor $g(E_m)$ since g should be a decreasing function and the argument decreases with time. We can obtain an estimate of the contribution to n from this factor with the assumption that the high-energy tail of the distribution is due to single scattering with Ne atoms and, furthermore, that the main mechanism for energy transfer is recoil of a single atom in the molecule. The distribution in energy transfer for an elastic collision between two atoms is proportional to $E^{-3/2}$ for a screened Coulomb atom-atom potential proportional to R^{-2}, where R is the distance between the colliding atoms [29], and this is probably a reasonable estimate. The variation for power-law potentials is between an E^{-2} dependence for the Coulomb potential and an E^{-1} dependence for infinite power (hard-sphere collisions) [29]. In order to apply equation (7) we must change to the variable $T_{e,m}$:

$$\frac{\mathrm{d}\ln g(E_m)}{\mathrm{d}\ln t} = \frac{\mathrm{d}\ln g(E_m)}{\mathrm{d}\ln E_m} \frac{\mathrm{d}\ln E_m}{\mathrm{d}\ln T_{e,m}} \frac{\mathrm{d}\ln T_{e,m}}{\mathrm{d}\ln t} \simeq -1.5 \frac{C(E_m) T_{e,m}}{E_m} \frac{-1}{G}. \tag{8}$$

The ratio CT/E is about 1.6 at around 1000 K (Fig. 6) but there are two small corrections to be included: the finite-heat-bath correction in the definition of $T_{e,m}$ (Eq. (3)) and the presence of a small amount of thermal excitation before collision induced excitation. Both tend to decrease the magnitude of the contribution to the power, which we then estimate to be about the same as in equation (7) but with the opposite sign. The end result is that the power should be very close to $n = -1$.

This estimate is in good accord with most of the observations shown in Figures 4 and 5 but for arginine in Figure 5c the slope is somewhat steeper than expected. It seems very unlikely that this is caused by loss of stored beam due to dynamic instability because all the ions were stored with the same ring parameters. Indeed, it is an important advantage of an electrostatic ring that these parameters do not depend on the mass of the ions. For glycine the logarithmic slope is significantly smaller than $n = -1$, and for alanine there seems to be a change to a smaller slope near 1 ms. Although there is some uncertainty in our estimates above, it is difficult to see that any of the factors considered can be responsible for these variations in n. In the following we discuss a possible explanation.

4.4 Competing fragmentation channels

The combination of Arrhenius parameters (E_d and v) for the dominant channel can be very different for different molecules and also, for example, for different charge states of the same molecule [10]. Moreover, it is well-known from studies of collision induced dissociation of biomolecules that usually there are many competing fragmentation channels, and that the relative abundance of fragment ions depends on the collision energy [30]. It therefore seems likely that there can be a temperature dependent competition between different fragmentation channels with quite different Arrhenius parameters.

If the rate constants for two fragmentation channels are equal at some excitation energy, the channel with the higher activation energy will dominate for higher excitation energies and the one with the lower activation energy (and smaller frequency v) will take over at lower excitation energies. For the formulas in equations (5, 6) this means that the last factor, which can be interpreted as the rms width of the weight function in equation (4), will increase and thus the logarithmic slope of the expression will be reduced.

This behaviour is illustrated by a model calculation in Figure 7. We have chosen two channels with a factor of two difference in the activation energy and with frequency factors adjusted to make the rate constants equal near a

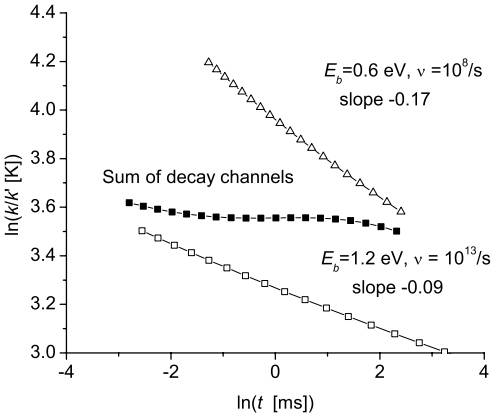

Fig. 7. Model calculation of the last term in equation (6) (divided by the heat capacity C) for two different Arrhenius decay rates and for the sum of the two rates. The slopes given in the figure are from linear fits and are close to the values given below equation (7). For the sum the slope is close to zero.

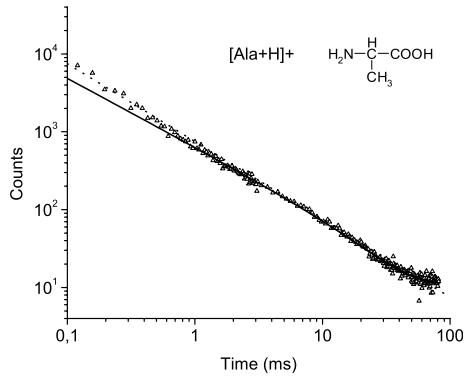

Fig. 8. Alternative fit to the decay curve for alanine, shown in Figure 5f, with the expression in equation (1) for $t > 1$ ms. The resulting parameters are $\delta = 0.12$ and $\tau = 16.6$ ms.

value of 10^3 s^{-1}. The abscissa in the plot is $\ln t$ and the ordinate is the logarithm of the rms width σ of the weight function in equation (4), $\sigma = (\mathrm{d}\ln k/\mathrm{d}T)^{-1}$, which for a rate constant expressed by an Arrhenius formula takes the form of the last factor in equation (6). For simplicity, the finite-heat-bath correction has been omitted in the calculation and it is then not necessary to specify the heat capacity.

The two curves with open triangles and squares correspond to rate constants determined by one of the two sets of parameters, while the filled squares give the result for a rate constant equal to the sum. With a single channel the slope is negative and it was estimated in equation (7) as $-2/G$. At $t = 1$ ms the values of the Gspann parameter are $G = \ln(10^5) = 11.5$ and $G = \ln(10^{10}) = 23$ and the estimate is seen to reproduce very well the numerically determined average slopes of the two curves, given in the figure. For the sum of the two channels the average slope is much smaller and there is a slight positive curvature. Thus the model supports the conjecture that the average logarithmic slope of the decay curve can be reduced when there is a competition between fragmentation channels with different activation energies.

In several of the decay curves in Figure 5 there is an indication of a change to a lower logarithmic slope around 1 ms. It is especially pronounced for alanine in Figure 5f. We have made an alternative fit to this measurement, with the function in equation (1) restricted to times $t > 1$ ms, and the result is shown in Figure 8. The fit in the restricted time region is much better than in Figure 5f and we now obtain a well-defined quenching time, $\tau = 16.6$ ms, which is consistent with the other values in Table 1.

For the decay curve for glycine in Figure 5e the slope is significantly lower than for the very similar molecule alanine (Fig. 5f). If the two curves are normalized to give the same level for the dissociation induced by rest gas collisions, the yield at short times is lower for glycine by about a factor of three. This could be due to a competition between fragmentation channels, as discussed above. An alternative interpretation could be that only a minor decay channel with rate constant k_1 is detected. The yield in equation (4) is then reduced by the factor $k_1(E_m)/k(E_m)$ which is time dependent [5,6]. However, such an interpretation seems excluded since we detect all neutral fragments.

4.5 Quenching by radiative cooling

We now turn to an explanation of the strong decrease of the intensity at $t \sim 10$ ms. It is very visible for some of the measurements, for example for phenylalanine in Figure 4, and almost invisible for others. The reason is that the relative contribution from fragmentation in gas collisions varies and can mask the reduction of the yield from unimolecular decay of hot ions.

The introduction of cooling into the description was discussed in reference [5] and in more detail in reference [18]. We give here a brief account with slightly different notation. We assume that the photon energies are so low that the effect of emission can be treated as continuous cooling of the molecule. This is certainly fulfilled for IR radiation from vibrations. The radiation power P_r varies slowly with temperature compared to the exponential dependence of the dissociation rate. Since we have observed the quenching by cooling over a narrow time range, only, we may ignore this variation and then to first order in t/τ_c express the cooling as

$$T(t) = T/(1 + t/\tau_c), \quad \text{with} \quad 1/\tau_c = P_r/CT. \qquad (9)$$

We let the symbols E and T_e denote the initial values of the energy and the effective decay temperature in equation (3), *i.e.*, the values at $t = 0$ before the cooling starts. The advantage of choosing these variables is that the distribution function $g(E)$ then changes only due to the depletion by decay. Instead of a time variation of T_e we then introduce the effect of cooling into equation (4) as a reduction of the decay rates for fixed E (and T_e). In analogy to equation (9), the denominator of the exponent in the Arrhenius expression is multiplied by a factor $(1+t/\tau_c')^{-1}$,

where τ_c' is slightly different from τ_c due to the finite-heat-bath correction, $\tau_c' = (T_e/T(0))\tau_c$. We then obtain

$$I(t) \simeq g(E_m)C(E_m)\int \mathrm{d}T_e v \exp\left(-\frac{E_d(1+t/\tau_c')}{k_B T_e}\right) \times \exp\left(-v\int_0^t \mathrm{d}t' \exp\left[-\frac{E_d(1+t'/\tau_c')}{k_B T_e}\right]\right) = g(E_m)C(E_m)\int \mathrm{d}T_e k(T_e)\mathrm{e}^{-Gt/\tau_c'} \times \exp\left(-k(T_e)G^{-1}\tau_c'\left(1-\mathrm{e}^{-Gt/\tau_c'}\right)\right). \quad (10)$$

We have here extracted from the integral the slowly varying energy distribution and the heat capacity stemming from the change of variable from E to T_e. Since G varies much more slowly with temperature than k it may be treated as a constant, and we find that there is a maximum of the integrand at an effective decay temperature $T_{e,m}$ corresponding to $k(T_{e,m}) = [G^{-1}\tau_c'(1-\exp(-Gt/\tau_c'))]^{-1}$. As before, E_m is the corresponding energy. The expression replacing equation (6) then becomes

$$I(t) \simeq \frac{1}{\tau(\exp(t/\tau)-1)} g(E_m)C(E_m)\frac{k_B T_{e,m}^2}{E_d}, \quad (11)$$

with $\tau = \tau_c'/G$. Equation (11) predicts a yield which follows the power law in equation (7) at short times, $t \ll \tau$, but is reduced exponentially by radiative cooling for $t \simeq \tau$. Comparison with equation (1) shows that we can identify τ with the quenching time determined by the experiment. In that equation the last three factors in equation (11) were represented by a power law, $(t/\tau)^\delta$, and according to our discussion above the power δ should be small, $\delta \sim \pm 0.1$. With an additive term representing fragmentation in collisions with the rest gas in the ring this function was seen to represent the data quite well and quenching times τ of order 10 ms were deduced. We discuss below the interpretation of the cooling as emission from IR-active vibrations.

4.6 Radiative cooling

Molecules and clusters couple to the radiation field both through IR-active vibrations and through the electronic degrees of freedom, while the coupling through rotations can normally be neglected because of their low frequencies. Transitions of electrons dominate at very high temperatures owing to their small mass but at low temperatures the electronic excitations "freeze out" and radiation from vibrations is most important. For molecules the transition temperature depends strongly on the magnitude of the energy gap between the highest occupied and the lowest unoccupied molecular orbital, and typically the transition takes place at 1000–1500 K [15]. For large metal clusters the gap is small and the plasma resonance of the free electrons dominates down to much lower temperatures [11–13].

Our earlier investigations of radiative cooling of ions stored in ELISA have been for systems cooled mainly by electronic radiation, metal clusters [5,27] and fullerenes at very high temperatures [5,17,18]. The heat radiation has also been observed directly for such systems and the spectrum was found to be broad and featureless like a Planck spectrum [31,32]. On the other hand, the radiation from C_{60} at temperatures below 1000 K consists mainly of the few characteristic lines from the IR-active vibrations [33]. For the amino acids studied here the temperature is not expected to exceed 1000 K and therefore emission from vibrations should dominate.

IR radiation from molecules has been investigated extensively in the past, in particular by Dunbar's group. A variety of techniques have been applied, for example delayed two-photon dissociation for isolated molecules (low pressure) [34]. If the photon energy is chosen such that the absorption of one photon does not lead to dissociation but the simultaneous absorption of two photons does, the dependence on the delay between the two photons reveals radiative cooling. A similar technique has been used for metal clusters [35]. The "lifetimes" for de-excitation by IR radiation from vibrations have typically been found to be in the range 0.1–1 s [16]. As we shall see below, the radiative de-excitation of an oscillator is exponential but usually this does not hold for molecules because several modes have large induced dipole moments and contribute to the radiation power [36].

We now quote the formula for the radiated power from a one dimensional harmonic oscillator (see, for example, Ch. 4 in [14]) and present an estimate of the lifetime. Classically, the power radiated from a charge q oscillating with cyclic frequency ω is given by

$$P_r = \frac{2\omega^4 q^2 \langle x^2\rangle}{3c^3} \quad (12)$$

in Gaussian units (in SI units q^2 should be divided by $4\pi\varepsilon_0$). The formula also applies for a quantum system if the mean square displacement from zero point vibrations is subtracted, *i.e.*, if $\langle x^2\rangle$ is replaced by $E/M\omega^2$, where M is the mass and E the excitation energy. This leads to the following formula for the power at temperature T,

$$P_r = \frac{2\omega^2 q^2}{3Mc^3}\frac{\hbar\omega}{\exp(\hbar\omega/k_B T)-1}, \quad (13)$$

where the last factor is the average excitation energy. Since the radiated power is proportional to this quantity, the energy will decrease exponentially for an isolated oscillator. The formula also shows that for fixed frequency the power is inversely proportional to mass and it illustrates the freeze-out of high-frequency transitions at low temperatures. On the other hand, the factor ω^2 implies that also the cooling by low-frequency vibrations (or rotations) is ineffective.

The first factor in equation (13) gives the reciprocal lifetime for de-excitation. To get a rough estimate we insert the elementary charge e as the effective charge q. The high frequency vibrations of the hydrogen atoms are at moderate temperatures little excited and we therefore apply an average mass of the heavy atoms, 14 amu. A typical photon energy is 0.2 eV, corresponding to a frequency

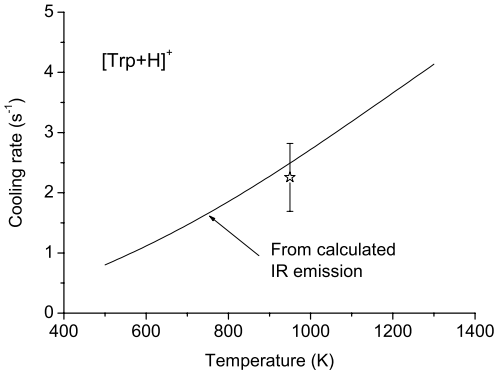

Fig. 9. Calculated radiative cooling rate P_r/CT for protonated tryptophan, compared with the rate derived from the measured quenching lifetime given in Table 1. A technical specification of the calculations is given in the text.

$\omega \simeq 3 \times 10^{14}$ rad/s, and we then obtain the lifetime 0.05 s for the exponential decrease of the oscillator energy. The cooling time τ_c was defined in equation (9) as the characteristic time for reduction of the temperature, not the energy, and hence we should multiply by the ratio CT/E which is of order two in the range 500–1000 K. The resulting value, $\tau_c \simeq 0.1$ s, is in good qualitative accord with the product of the measured quenching times, $\tau \sim 10$ ms, and a Gspann parameter $G \sim 20$, considering that many vibrations are not IR active ($q \sim 0$).

4.7 Comparison with calculation for tryptophan

As an example, we have carried out detailed calculations for protonated tryptophan. The structure was optimised at the B3LYP/ 6-31+G(d) level of density functional theory with the Gaussian 98 package [37]. All calculated frequencies are real, which confirms that the stationary point is a local minimum on the potential energy surface. The resulting caloric curve was presented in Figure 6. In addition to the frequencies also the IR intensities were calculated from the dipole derivatives, which replace the square root of the factor q^2/M in equation (13). The most intense IR band is due to CO stretch (1812 cm^{-1}). Also OH stretch (3653 cm^{-1}) and NH stretch (NH_3^+ group, 3200–3500 cm^{-1}) vibrations are highly IR active. The same is true for NH bending (NH_3^+ group, 1493 cm^{-1}) and OH bending (1195 cm^{-1}). We have not applied any empirical scaling of the frequencies. The resulting cooling rate $1/\tau_c$ defined in equation (9) is shown as a function of temperature in Figure 9.

In order to compare with the measured quenching time given in Table 1 we need the value of the Gspann parameter for the decay. We have observed that the dominant decay channel after collisional excitation of protonated tryptophan produces the immonium ion $^+NH_2CHCOOH$. We have carried out an analogous calculation for this ion and for the remaining fragment, and have then calculated the energies of the three molecules at the B3LYP/6-311+G(2d,p) level and corrected for zero-point motion [non-scaled B3LYP/6-31+G(d) values]. The result is a predicted dissociation energy of $E_d = 1.5$ eV. With the assumption that the reverse barrier in the reaction is negligible we can use this value in the Arrhenius formula in equation (2).

Finally, we have estimated the decay rate at a well defined energy from a measurement of laser induced fragmentation in ELISA. After absorption of fourth harmonic photons from a Nd:YAG laser in the upper side of the ring in Figure 1 a large yield of fragmentation was observed during the first passage of the other side of the ring, and we estimate that the lifetime is in the range 5–15 μs. From observation of a linear dependence on laser power we conclude that the signal results from absorption of a single photon, which gives a total excitation energy of 4.95 eV, including the thermal energy at room temperature. The frequency factor in the Arrhenius formula is then calculated to be $v \sim 2 \times 10^{11}$ s^{-1}. From the relation $k(t) \sim 1/t$ for the power-law decay we obtain for the Gspann parameter at 17 ms, $G = \ln(vt) \sim 22$, and for the decay temperature, $T_e = E_d/k_B G \sim 800$ K, corresponding to an internal temperature of $T \sim 950$ K according to equation (3).

With these parameters the cooling rate has been calculated from our measured quenching rate and, as shown in Figure 9, there is excellent agreement with the theoretical calculation. The experimental uncertainty is indicated by the error bar but there is also a considerable uncertainty in the theoretical calculation, stemming mainly from the evaluation of the dipole derivatives. It is interesting to note that it is not possible to investigate radiative cooling of tryptophan by experiments with single-photon excitation. The absorption band of the aromatic ring in the side chain extends only to wavelengths of order 300 nm, corresponding to energies above 4.4 eV. As seen in Figure 6 this corresponds to temperatures well above 950 K, where cooling becomes important.

We have not made a detailed analysis for the other amino acids, but the situation must be similar. Their heat capacities are smaller (see the mass numbers in Tab. 1), and for the molecules without an aromatic ring the lowest absorption band is at even shorter wavelengths. Hence these molecules will also be too hot after absorption of a single photon for radiative cooling to be important. Since the IR active vibrations in tryptophan, CO, OH and NH stretch vibrations etc., are present in all the amino acids it is expected that the cooling rates will be similar. This is in good accord with our finding of very similar quenching times for the amino acids selected in this study.

5 Concluding remarks

In recent years a number of studies of the dynamics of molecular ions in storage rings have demonstrated that such rings can be a useful supplement to other storage facilities, like ICR (Ion Cyclotron Resonance) traps [38,39], for the study of gas phase chemistry. We have here focussed on measurements on molecules with a broad distribution in excitation energy, and have chosen representative examples of amino acid cations. The results confirm

the approximate $1/t$ decay law we have demonstrated previously for cluster ions. A strong reduction of the yield relative to the power law for times longer than about 10 ms has been observed, and in accordance with our earlier studies it has been interpreted as quenching by radiative cooling.

The most important result of the experiments is the determination of the quenching times τ. It may be argued that for measurement of radiative cooling our method is rather indirect because it requires a determination of the Arrhenius parameters for the decay to translate the quenching time into a characteristic cooling time. On the other hand, the quenching time is an important quantity in its own right. Radiative cooling can give significant corrections in determinations of dissociation energies when the time scale of experiments is not very short compared with the quenching time [27,40].

The observed power-law spectra for times shorter than τ give indications of a temperature dependent competition between different fragmentation channels, and we plan to investigate this idea by experiments with stored ions excited to a well defined energy with a laser pulse of variable wavelength. For this purpose we shall install a linear Paul trap for bunching, with better control of the ion temperature and with better pumping outside the trap to reduce excitation by gas collisions after extraction.

This investigation was supported by a grant from the Danish National Research Foundation to the research centre ACAP (**A**arhus **C**enter for **A**tomic **P**hysics). The collaboration was initiated by the European network LEIF, contract HPRI-CT-1999-40012, and has been supported also by the EU Research Training Network, contract HPRN-CT-2000-0002, and by an EU grant to ISA (**I**nstitute for **S**torage ring facilities, **A**arhus) for Transnational Access to Major Research Infrastructures, contract HPRI-CT-2001-00122. SBN acknowledges the Danish Natural Science Research Council for a Steno grant (# 21-02-0129).

References

1. J.H. Klein-Weile, P. Simon, H.-G. Rubahn, Phys. Rev. Lett. **80**, 45 (1998)
2. M. Simon, F. Träger, A. Assion, B. Lang, S. Voll, G. Gerber, Chem. Phys. Lett. **296**, 579 (1998)
3. J.U. Andersen, P. Hvelplund, S.B. Nielsen, U.V. Pedersen, S. Tomita, Phys. Rev. A **65**, 053202 (2002)
4. P.B. Armentrout, Int. J. Mass Spectrom. **200**, 219 (2000)
5. K. Hansen, J.U. Andersen, P. Hvelplund, S.P. Møller, U.V. Pedersen, V.V. Petrunin, Phys. Rev. Lett. **87**, 123401 (2001)
6. K. Hansen, O. Echt, Phys. Rev. Lett. **78**, 2337 (1997)
7. D. Thölmann, D.S. Tonner, T.B. McMahon, J. Phys. Chem. **98**, 2002 (1994)
8. R.C. Dunbar, T.B. McMahon, D. Thölmann, D.S. Tonner, D.R. Salahub, D. Wei, J. Am. Chem. Soc. **117**, 12819 (1996)
9. W.D. Price, P.D. Schnier, R.A. Jockush, E.F. Strittmatter, E.R. Williams, J. Am. Chem. Soc. **118**, 10640 (1996)
10. D.J. Butcher, K.G. Asano, D.E. Goeringer, S.A. McLuckey, J. Phys. Chem. A **103**, 8664 (1999)
11. U. Kreibig, M. Vollmer, *Optical Properties of Metal Clusters* (Springer, Berlin, 1995)
12. W.A. de Heer, K. Selby, V. Kresin, J. Masui, M. Vollmer, A. Chatelain, W.D. Knight, Phys. Rev. Lett. **59**, 1805 (1987)
13. C. Ellert, M. Schmidt, C. Schmitt, T. Reiners, H. Haberland, Phys. Rev. Lett. **75**, 1731 (1995)
14. J.U. Andersen, E. Bonderup, Eur. Phys. J. D **11**, 413 (2000)
15. P. Boissel, P. de Parseval, P. Marty, G. Lefèvre, J. Chem. Phys. **106**, 4973 (1997)
16. R.C. Dunbar, Mass Spectr. Rev. **11**, 309 (1992)
17. J.U. Andersen, C. Brink, P. Hvelplund, M.O. Larsson, B. Bech Nielsen, H. Shen, Phys. Rev. Lett. **77**, 3991 (1996)
18. J.U. Andersen, C. Gottrup, K. Hansen, P. Hvelplund, M.O. Larsson, Eur. Phys. J. D **17**, 189 (2001)
19. S.P. Møller, Nucl. Instrum. Meth. A **394**, 281 (1997)
20. J.U. Andersen, P. Hvelplund, S. Brøndsted Nielsen, S. Tomita, H. Wahlgreen, S. Pape Møller, U.V. Pedersen, J.S. Forster, T.J.D. Jørgensen, Rev. Sci. Instrum. **73**, 1284 (2002)
21. K.G. Asano, D.J. Butcher, D.E. Goeringer, S.A. McLuckey, J. Mass Spectrom. **34**, 691 (1999)
22. N. Bohr, Nature **137**, 344 (1936)
23. V. Weisskopf, Phys. Rev. **52**, 295 (1937)
24. D.H.E. Gross, P.A. Hervieux, Z. Phys. D **35**, 27 (1995)
25. K. Hansen, Philos. Mag. B **79**, 1413 (1999)
26. J.U. Andersen, E. Bonderup, K. Hansen, J. Chem. Phys. **114**, 6518 (2001)
27. J.U. Andersen, E. Bonderup, K. Hansen, J. Phys. B: At. Mol. Opt. Phys. **35**, R1 (2002)
28. C.E. Klots, Z. Phys. D **21**, 335 (1991), and references therein
29. J. Lindhard, V. Nielsen, M. Scharff, K. Dan. Vid. Selsk. Mat. Fys. Medd. **36**, 10 (1968)
30. I.O. Papayannopoulos, Mass Spectr. Rev. **14**, 50 (1995)
31. U. Frenzel, U. Hammer, H. Westje, D. Kreisle, Z. Phys. D **40**, 108 (1997)
32. R. Mitzner, E.E.B. Campbell, J. Chem. Phys. **103**, 2445 (1995)
33. C.I. Frum, R. Engleman Jr, H.G. Hedderich, P.F. Bernath, L.D. Lamb, D.R. Huffman, Chem. Phys. Lett. **176**, 504 (1991)
34. R.C. Dunbar, J.H. Chen, H.Y. So, B. Asamoto, J. Chem. Phys. **86**, 2081 (1986)
35. C. Walther, G. Dietrich, W. Dostal, K. Hansen, S. Krückeberg, K. Lützenkirchen, L. Schweikhard, Phys. Rev. Lett. **83**, 3816 (1999)
36. R.C. Dunbar, J. Phys. Chem. **90**, 7369 (1989)
37. M.J. Frisch *et al., Gaussian 98, Revision A.7*, Gaussian Inc., Pittsburgh PA, 1998
38. L. Thorne, J.L. Beauchamp, in *Gas Phase Chemistry*, edited by M.T. Bowers (Academic, Orlando, Fl., 1984), Vol. 3
39. M.F. Jarrold, Annu. Rev. Phys. Chem. **51**, 179 (2000)
40. C. Lifshitz, Int. J. Mass Spectrom. **198**, 1 (2000)